PC Desktop Aerodynamic Models for Store Separation from Weapons Bay Cavities and Related Vortical Processes

Norman Malmuth
Project Manager and Senior Scientist
Rockwell Science Center, P.O. Box 1085
1049 Camino Dos Rios, Thousand Oaks
CA 91360, USA

A. Fedorov and V. Shalaev
Associate Professor, Moscow Institute
of Physics and Technology
16 Gagarin Street, Zhukovski
Moscow Region 1401 80
Moscow, Russia

J. Cole
Former Margaret Darrin Professor
Rensselaer Polytechnic Institute
(deceased, 1999)

M. Hites and D. Williams
Professor, Illinois Institute of Technology
Chicago, Illinois, USA

Abstract

Combined asymptotics and numerics (CAN) give an insightful picture of shear layer cavities and provide a means of quickly visualizing the flow pattern within them. It appears that the recirculating flow can be modeled with inviscid approximations of the viscous flow for many practical cases. For bodies transiting the shear layer of such cavities such as in store separation, much of the details such as the modification of the apparent mass effect due to the shear layer can be obtained from cross flow approximation-inner solutions from slender body theory. These tools are now being extended to transonic flows.

1. Need for store separation work

Air-launched weapons is an essential military technology that can provide strategic and tactical supremacy. Emphasis on safe, high-accuracy, reliable store separation will be critical for weapon system upgrades to cost-effectively meet threats in a financially austere environment for new aircraft development for the foreseeable future. Although the problem of weapons release from an aircraft platform has received much attention, more effort is needed to understand the underlying basic physics and essential parameters. In a larger sense, this technology is a subset of the problem of the interactions between moving bodies in all speed ranges. Applications include separation and carriage of various stage vehicles for space missions and flight testing as well as crew escape. For this group, hypersonic multistage vehicle concepts of interest to the U.S. Air Force frequently utilize the launch of a small rocket-powered stage from a large subsonic or transonic aircraft such as the B-52. Other examples are the PEGASUS series and the Shuttle. Currently, multistage launch scenarios are envisioned for future hypersonic and space applications. A new thrust involves the use of airbreathing (scramjet or turbo-scramjet) rather than rocket-powered stages.

Many of the previous investigations of store separation have been confined to external store carriage. Comparatively less attention is being given to separation from cavities and bays. This is probably due to the additional complications related to the interaction of the store with the shear layer and the store as well as the coupling with the walls of the

Paper presented at the RTO AVT Symposium on "Advanced Flow Management: Part A – Vortex Flows and High Angle of Attack for Military Vehicles", held in Loen, Norway, 7-11 May 2001, and published in RTO-MP-069(I).

Report Documentation Page

Form Approved
OMB No. 0704-0188

1. REPORT DATE	2. REPORT TYPE	3. DATES COVERED
00 MAR 2003	**N/A**	**-**

4. TITLE AND SUBTITLE	5a. CONTRACT NUMBER
PC Desktop Aerodynamics Models for Store Separation from Weapons Bay Cavities and Related Vortical Processes	5b. GRANT NUMBER
	5c. PROGRAM ELEMENT NUMBER
6. AUTHOR(S)	5d. PROJECT NUMBER
	5e. TASK NUMBER
	5f. WORK UNIT NUMBER
7. PERFORMING ORGANIZATION NAME(S) AND ADDRESS(ES) **NATO Research and Technology Organisation BP 25, 7 Rue Ancelle, F-92201 Neuilly-Sue-Seine Cedex, France**	8. PERFORMING ORGANIZATION REPORT NUMBER
9. SPONSORING/MONITORING AGENCY NAME(S) AND ADDRESS(ES)	10. SPONSOR/MONITOR'S ACRONYM(S)
	11. SPONSOR/MONITOR'S REPORT NUMBER(S)

12. DISTRIBUTION/AVAILABILITY STATEMENT
Approved for public release, distribution unlimited

13. SUPPLEMENTARY NOTES
Also see: ADM001490, Presented at RTO Applied Vehicle Technology Panel (AVT) Symposium held inLeon, Norway on 7-11 May 2001, The original document contains color images.

14. ABSTRACT

15. SUBJECT TERMS

16. SECURITY CLASSIFICATION OF:			17. LIMITATION OF ABSTRACT	18. NUMBER OF PAGES	19a. NAME OF RESPONSIBLE PERSON
a. REPORT	b. ABSTRACT	c. THIS PAGE			
unclassified	**unclassified**	**unclassified**	**UU**	**20**	

cavity. Many of the large-scale computational simulations have focused on acoustic interactions with the cavity and the associated structural loadings on the fins of the guidance avionics. Much of these large amplitude oscillations are associated with traveling waves along the shear layer and their interaction with recirculating cavity flow. By contrast to the empty cavity, the filled cavity poses other challenges. The three phases of the motion, above, across and below the shear layer involve special combined dynamics and aerodynamic problems.

2. Physics and modeling issues

Figure 1 shows the various phases of a weapons-bay store release. These are:

A) Internal regime in which the store is well within the cavity.

B) Transitional regime in which the store is transiting the shear layer.

C) External flow regime in which the store is outside the cavity but still influenced by it.

Inside the cavity, high-amplitude oscillations of the recirculating flow occur. In spite of these amplitudes, the inertia of the store is such that the average effect is nulled out and the dominant physics is the interaction of the store with the layer. While the store is in the cavity, the interaction with the walls can be significant if the wall dimensions are comparable to the store's. As the store crosses the shear layer, three subcases can be distinguished. If τ is the thickness ratio of the store and δ is the shear layer thickness, these are

i. $\frac{\delta}{\tau} \to 0$

ii. $\frac{\delta}{\tau} = O(1)$

iii. $\frac{\delta}{\tau} \to \infty$

Case (i) is a practical limit at typical flight Reynolds numbers. Accordingly, it has been a primary focus of our research. It is also the simplest of the three. Nevertheless, it presents many mathematical challenges. Foremost are the possibility of nonlinear boundary conditions that occur on the shear layer. These result from specification of equality of pressure across the shear layer between the cavity and the external flow. For practical situations involving high fineness ratio almost cylindrical bodies the nonlinearities can be reasonably approximated as second order and giving a much simpler boundary condition. Within the initial emphasis of determining parameters that control safe separation, unsteady processes such as traveling vortices, edge tones, shear layer impingement phenomena and instabilities, as well as bifurcating "flapping" states that are important for store-fin structural integrity, were suppressed in favor of understanding the structure of the time-averaged cavity flow. The latter is critical for safe separation, assuming fin survival. Figure 1 shows supporting estimates that strongly suggest that although violent short-period acoustic oscillations occur inside the shear layer, the inertia of the store is so large that its motion is primarily controlled by rigid-body aerodynamics.

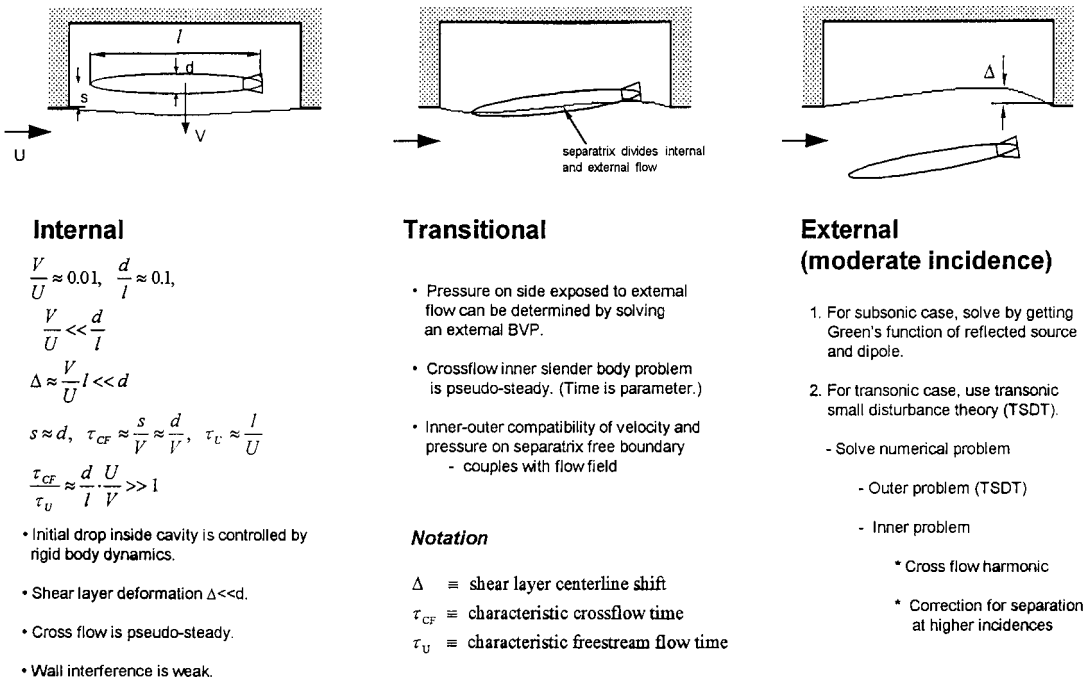

Fig. 1 Store separation from a weapons-bay cavity, motion phases.

3. Empty cavity flows

To treat the empty cavity, we exploited several simplifications that we believe accurately reflect the true physics of the problem. Case (i), enumerated above, gives a systematic asymptotic structure in which the shear layer in an outer expansion approximation looks like a vortex sheet. As a first implementation of this concept , the interaction of the vortex sheet with the cavity flow was worked out for a two-dimensional cavity.

The "outer" background flow field of the empty cavity flow was determined from an eigenfunction approach to model the cavity core flow in an inviscid approximation. This flow was matched with a Blasius free shear layer simulating the interaction of the "inner" cavity flow with the external flow. Formal matching gave us a consistent approximation scheme for our domain-decomposition solution method. An output of the matching was to provide boundary conditions for the outer recirculating flow. Because of its slow speed, the dominant approximation is harmonic. To our knowledge, this is the first time such a procedure has been used for such a problem.

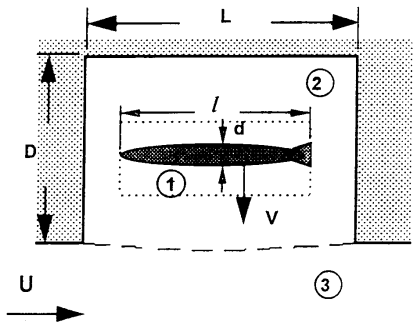

Basic constraints:

- **Body speed V<<U**
- **Thin body: d/l<<1**
- **Cavity depth D>>d**

1. Viscous forces small compared to gravitational.

$$\Pi = \frac{\text{Gravitational speed at distance D}}{\text{Induced vertical velocity from mixing layer}} = \frac{V}{V_{mix}} \approx \frac{\sqrt{2gD}}{U\delta'(x)} \approx \frac{\sqrt{2gD\,\mathrm{Re}}}{U}$$

For $g = 10$ m/s, $\mathrm{Re} = 10^6$: (typical for fighters)

U m/s	Π	speed
100	40	subsonic
300	10	transonic

2. 3-D effect is weak.

Since d/l<<1, cross-flow $(v_1, w_1) \approx V >> u_1 \approx l' \frac{d}{l}$

flow field near the body is approximately 2-D in cross flow planes.

3. Wall interaction effect is weak.

Since cross region scale d<<D, bottom wall interference is weak.

Since $u_1 << V$, side wall interference is weak.

Fig. 2 Store in cavity.

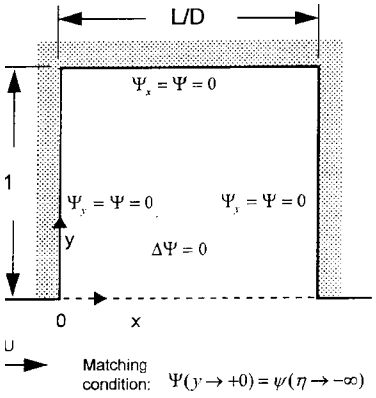

Inviscid stream-function in cavity region:

$$\Psi \equiv \frac{\Psi^*}{U^* D^*} = 2a \sum_{n=1}^{\infty} \frac{sh(n\pi a(1-y))\sin(n\pi x)}{sh(n\pi a)} \int_0^{L/D} \delta(x')\sin(n\pi x')dx'$$

$a = D/L$

$\delta =$ shear layer thickness

For Blasius shear layer:

$$\Psi \equiv \frac{\Psi^*}{U^* D^*} = \frac{2af(-\infty)}{\sqrt{\mathrm{Re}_D}} \sum_{n=1}^{\infty} \frac{sh(n\pi a(1-y))\sin(n\pi x)}{sh(n\pi a)} \int_0^{L/D} \sqrt{x'}\sin(n\pi x')dx'$$

Fig.3 Eigenfunction solution of empty cavity flow field.

Figure 2 illustrates a system which was used to implement this approach. To illustrate its power, the aforementioned matched asymptotic approach was used to compute the recirculating eddy flow in the empty shear layer. Figure 3 summarizes and solves the related boundary value problem for the stream function Ψ accounting for matching with the viscous shear layer which in the outer limit appears as a vortex sheet of the cavity flow. A convergent eigenfunction function expansion has been obtained for the empty two-dimensional laminar shear layer cavity flow. The streamline topology determined obtained from a 5 minute desktop PC run closely resembles that from from 15 hour CDC 205 runs for a 3-D turbulent shear flow cavity as shown in Fig. 4. An important stagnation singularity at the downstream wall allows a steady state recirculating eddy

structure. Understanding the loads imposed on a store from this vortex will be critical in assessing safe separation and store certification for all three services. The structure of this solution is provides a launching pad for computing the filled cavity flow. Coupling this with the latter has given us new insights into the key lumped dimensionless groups controlling the safe store separation phenomenon to complement qualitative inferences from large-scale CFD runs.

During the formulation of the problem shown in Fig. 3, considerations such as those indicated in Fig. 2 illuminated lumped nondimensional parameters such as that expressing the ratio of gravitational to viscous forces. These can be used for experimental design and scaling. Estimates based on such parameters show that when the store is inside the cavity, a flow regime can occur for which

- gravitational forces dominate, and the initial drop phase of the store is controlled primarily by ***rigid body dynamics***.
- the shear layer deformation is small compared to the store thickness.
- the cross flow is pseudo-steady.
- the interaction of the body with walls is weak

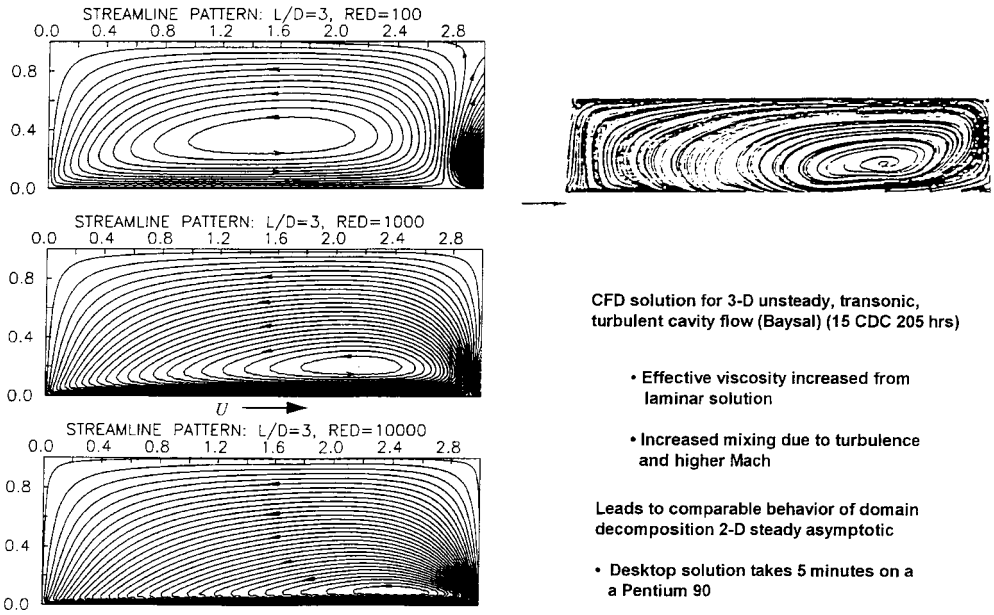

Fig.4 Comparison of CAN (IA) and CFD solutions for shear layer-driven cavity flow.

4. Flat plate interaction with shear layer

One of our recent activities was focused on modeling the coupled fluids and dynamics problem of a wing-like shape separating from a cavity. This work was a prelude to numerical implementation as well as studying the physics of bodies of revolution and more complicated bodies such as combined bodies and fins. This effort is to provide new insights into these basic physical processes to complement current large-scale CFD simulation efforts. With our combined asymptotic and numerical framework, the following unit problems have been formulated:

(A) Body moves inside cavity (internal regime)

(B) Body is transiting the shear layer between the cavity and external flow (transitional regime)

(C) Body moves outside the cavity (external regime)

These problems have been studied using asymptotic methods which lead to drastic reduction of the problem size from large-scale computationally-intensive CFD approaches.

For the internal and external regimes, forces and moments on a slender body inside and outside a 3-D rectangular cavity closed-form representations have been obtained. For the transitional regime, interaction between a discontinuous inviscid approximation to the shear layer and a thin low aspect ratio delta wing has been analyzed. Lumped nondimensional parameters that control interaction between the body and shear layer have been identified. Formulations were made for various distinguished limits in the transitional regime involving the relative size of body angle of attack, slenderness (e.g., span to chord ratio and other parameters). We have obtained approximate analytical solutions for the flow field, pressures, forces and moments for many of these cases.

As indicated by Wright Labs A*f*SIM, simplified modeling of these processes is essential to develop control methods to assure safe store separation from weapons bay cavities. They are also critically important in assessing the safe separation and Circular Error Probability (CEP) targeting accuracy impact of noise and vibration alleviation methods such as pulsed blowing and spoilers for weapons bays. These are frequently devised to disrupt the destructive interaction between recirculating eddy structures and shear layer instabilities.

Figure 5 illustrates the appropriate boundary value problem for the inner expansion perturbation velocity potential for an almost rectangular flat plate slender wing of span b dropping under gravity below a shear layer y direction (in regime (C)). Here, the displacement quantity $Y(t)$ denotes the normalized distance of the plate from the shear layer. In addition to the boundary conditions shown, the perturbation potential behaves like Z^{-1} as $Z \to \infty$, where $Z = z + iy$ and all lengths are scaled by the span b where $b \to 0$. Details of this analysis will be provided elsewhere. Only the main points will be mentioned here.

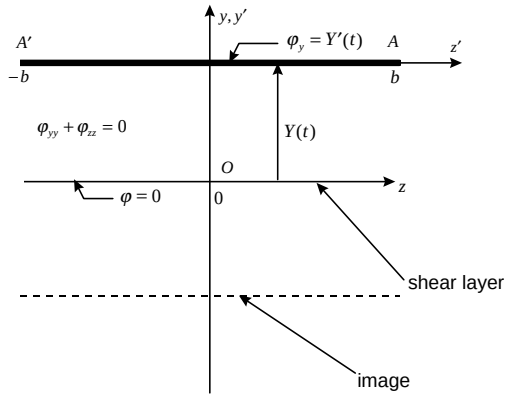

Fig.5 Crossflow "biplane problem" for plunging plate.

Important special cases connected with pure plunge (zero angle of attack) have been investigated. Combined limits based on a time scale which is the square root of the span divided by the acceleration of gravity g (the time for the lifting surface to drop its own span b) have been identified. These limits involve the small parameter ε which is the dimensionless span in units of the wing chord L and the Froude number F, where if $U =$ freestream velocity then $F = \sqrt{\dfrac{U}{gL}}$. The occurrence of the Froude number F underscores the resemblance of the flow physics (in some respects) to those occurring in water entry and impact problems such as those of underwater missiles, seaplane landing and skip-bombing in World War II. To our knowledge, this important connection has apparently never been previously recognized. It should be noted that important dissimilarities exist since although sudden differences in forces occur across an interface, in the hydrodynamic case, the interface divides two media of greatly different density. In the weapons-bay store application, the interface is roughly a tangential velocity discontinuity with no density discontinuity across it.

In an important limit involving high F and $\varepsilon \to 0$, the nonlinear boundary conditions on the shear layer can be linearized to its undistorted position and its shape is a passive scalar that can be determined from the flow tangency condition ***after*** the flow field is solved. Although this problem also yields an integral equation, we have shown that this complexity can be bypassed by using a conformal mapping similar to that appearing in the theory of biplanes which involves elliptic functions and integrals characterizing a Schwarz-Christoffel transformation.

Here the inner time scale is related F. Since the flow is incompressible, the unsteady effect is related to the time derivative of the potential appearing in the unsteady Bernoulli equation as well as the parametric dependence of the boundary conditions on time shown in Fig. 5. The incompressible assumption is made for convenience as a stepping stone to transonic future effort in which the transonic and incompressible inner near field boundary value problems both have a similar ***implicit*** steady structure with the time t entering parametrically. The incompressible assumption is also of direct relevance to airdrop applications.

The aerodynamics is coupled to the dynamics through the plate dynamical equation of motion

$$Y''(t) = 1 - \frac{L}{W} = 1 - CY'(t)\, f(Y)\,, \tag{1}$$

where L is the lift on the plate and W is its weight. The lift is given by

$$L = c_1 \int_0^b \varphi\big(z, Y(t)\big) dz\,, \tag{2}$$

where c_1 is a constant independent of y and z, and the function $f(Y)$ is proportional to the lift L.

The solution of the boundary value problem shown in Fig. 5 arises in biplane theory (*cf.* [1]) and allows us to evaluate the integral in (2). This is in terms of elliptic functions and integrals* that will be detailed elsewhere. What is new is the association of this boundary value problem with a flat plate separation from a shear layer. We are not aware of this connection having been made before. As indicated previously, the homogeneous Dirichlet condition expressing continuity of the pressure from the cavity to that of the external flow across the shear layer $y = 0$ only applies if $b'(x)$=0, where x is in the streamwise direction. Otherwise, a mathematically interesting nonlinear boundary condition arises involving the squares of the crossflow velocities on the shear layer as previously indicated.

Certain other restrictions on the slope of the body, if relaxed make the subsonic problem more nonlinear in that the shear layer becomes a truly free boundary in that its position is no longer at $y = 0$, but interacts with the solution for φ. This invalidates the reflection procedure used here. We conjecture that these complications may not substantially alter the qualitative features of the solution that we discuss here. Coupling the dynamics and the aerodynamics gives an unique and interesting initial value problem for the trajectory $Y(t)$. This consists in solving (36) subject to the initial conditions

$$\left.\begin{aligned} Y(0) &= 0 \\ Y'(0) &= v_0 \end{aligned}\right\} \tag{3}$$

where the initial velocity v_0 is associated with the drop through the cavity. It is interesting to note that the coupling between the dynamics and aerodynamics is associated with the nonlinear term $CY'f(Y)$ in (1) which is determined as a passive scalar. To our knowledge, this type of decoupling of the otherwise complicated interaction has also not been previously developed. In [1], $f(Y)$ was only computed in a limit of small Y because of the unavailability of computers at the time of this early work. Fig. 6 shows the variation of the normalized lift, which is half of its large-time asymptotic appropriate to no shear layer interaction in the freestream. This is because the side facing the cavity experiences ambient pressure just as the plate crosses the shear layer, while that exposed to the freestream has the elliptic pressure loading that would have existed on the bottom face of a plunging plate in an infinite flow without a shear layer.

---

*A different approach using elliptic theta functions and Cauchy integrals is indicated in [2] for flat bodies and bodies of revolution.

Because of the strong nonlinearity, even the simple looking Eq. (36) had to be solved numerically. In fact, it exhibited stiff properties, due to the "boundary layers" at $t = 0$ and ∞.

Figure 7 shows the effect of the nonlinearities and the coupling of the lift and the drop trajectory for large values of the ballistic parameter L/W.

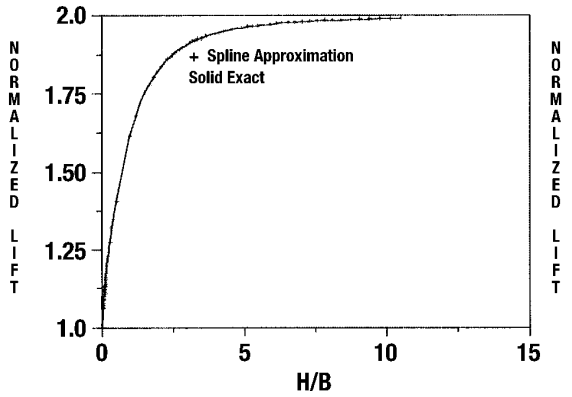

Fig 6 Shear layer interference lift inteference function (*f(y)*=normalized lift ordinate), $H/B \equiv Y/b$.

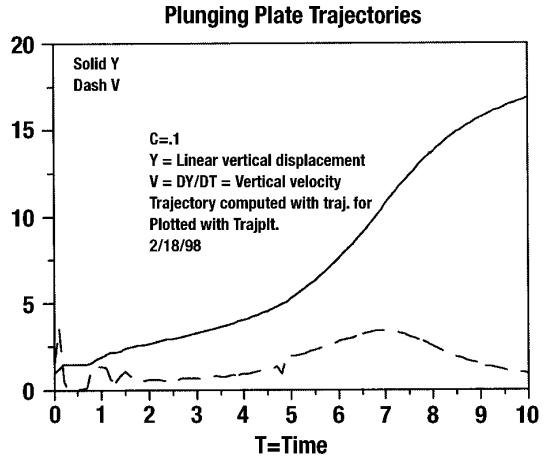

Fig.7 Plunging plate trajectories.

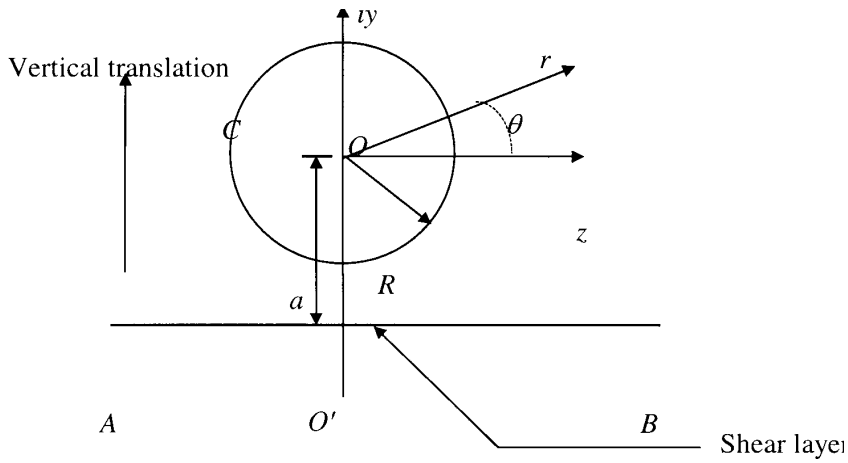

Fig.8 Vertically translating cylinder in crossflow plane with local polar coordinate system.

5. Bodies of revolution interacting with shear layers

A close-up of the boundary value problem for the near field of a plunging cylinder in proximity to a shear layer generated by a cavity adjoining an incompressible flow is shown in Fig. 8. ***This problem is almost identical to the dominant order transonic inner problem.*** Without the shear layer present, the exterior Neumann problem for the inner perturbation velocity potential φ with Neumann data given

$$\varphi_{\tilde{r}}(x, R, \tilde{z}) = \tilde{Y}'(\tilde{t})\sin\theta \tag{4}$$

where $\tilde{Y}'(\tilde{t})$ is the plunging velocity and t is a Froude normalized time. For slender bodies, $\varphi_{\tilde{y}\tilde{y}} + \varphi_{\tilde{z}\tilde{z}} = 0$ and $\varphi \to 0$ as $\tilde{r} \to \infty$. This matches with a streamwise line doublet* inner representation of an outer solution is solved by a crossflow doublet at the origin O', since the distance a in outer coordinates is negligible.

The complex potential $F(Z) = \varphi + i\psi$, where $Z = z' + iy'$ are relative to the origin O shown in Fig. 8 which satisfies the condition that φ =0 on the shear layer, AB is

$$F = iC\left\{\frac{1}{Z - ia} + \frac{1}{Z + ia}\right\}. \tag{5}$$

Note that the introduction of the image term in (5) to satisfy the homogeneous boundary condition

$$\varphi(z,0) = 0 \tag{6}$$

"spoils" the Neumann boundary condition (4). A second order correction must be made by re-imaging the doublet image by inversion into the circle in the upper half plane. Continuing this process gives an infinite set of images. This generates an asymptotic

* This is similar to that used in the first two authors' work on wind tunnel wall interference theory.

expansion in the parameter $\frac{R}{a}$ which holds in the limit $\frac{R}{a} \to 0$. This structure is clarified by referring quantities to the origin at O and introducing the new variable $w = Z - ia$ so that with the first correction to the complex potential is

$$F = iC\left\{\frac{1}{w} + \frac{1}{w+2ia}\right\}. \tag{7}$$

This gives the complex velocity

$$F'(w) = -iC\left\{\frac{1}{w^2} + \frac{1}{(w+2ia)^2}\right\}. \tag{8}$$

By (8) and

$$\frac{\partial\varphi}{\partial r} = \mathrm{Re}\left\{F'(w)\frac{\partial w}{\partial r}\right\}, \tag{9}$$

we obtain

$$\frac{r}{C}\frac{\partial\varphi}{\partial r} = \mathrm{Im}\left\{\frac{1}{w} + \frac{w}{(w+2ia)^2} + \cdots\right\}. \tag{10}$$

For a general sequence of reflections in which

$$F = iCf(w, w-a_1, w-a_2, w-a_3, \ldots),$$

where the location of the doublet reflection points are at $a_i,\ i = 1,2,3\ldots$ [*]

$$\frac{\partial\varphi}{\partial r} = \mathrm{Re}\left\{iCf'(w)e^{i\theta}\right\}. \tag{11}$$

From these relations it is clear that

$$C = -R^2. \tag{12}$$

It appears that successive corrections for the shear layer B.C. and the cylinder B.C. each of which is diminishingly spoiled by the last image appears to give a divergent series. However, this is typical of asymptotic expansions in which the optimum number of terms can be one or two! Equation (10) can be interpreted in this way so that as $\frac{R}{a} \to 0$

$$\frac{\partial\varphi}{\partial r} = \frac{R^2}{r}\left\{\frac{1}{w} + O\left(\frac{R}{a}\right)\right\} \tag{13}$$

[*] Note that the reflections in the circle involve changing the strength of the doublet. See Milne-Thompson, *Hydrodynamics*, 3rd ed., ¶ 8.81, p. 217.

Numerical studies show that (4) is satisfied by (13), even for $\frac{R}{a}$ of the order of 0.5. Even $\frac{R}{a}$ near unity appears to be a reasonable approximation. In the future effort, the off-boundary robustness of the two-term asymptotic as an approximation to the solution will be explored. To compute the linear trajectory of the body, the following equation holds in normalized coordinates

$$Y''(t) = 1 - \frac{L}{W}, \tag{14}$$

where L is the lift and W is the weight. Defining a lift coefficient as

$$C_L = \frac{L}{\frac{1}{2}\rho U^2 l^2},$$

where l is the store length, and a pressure coefficient

$$C_p = \frac{P - P_\infty}{\frac{1}{2}\rho U^2},$$

then since

$$C_p = -2\delta^2 \varphi_t,$$

the one-term asymptotic expression for C_L is

$$C_L = -8\left(\frac{\delta}{l}\right)^2 \int_0^{\pi/2} \varphi_t(R,\theta)\, d\theta = 2\left(\frac{\delta}{l}\right)^2 R^2 \tilde{Y}''(\tilde{t})$$

where the doublet solution is used to obtain

$$\varphi = C\frac{\sin\theta}{\tilde{r}} \tag{15}$$

Since the lift is proportional to the acceleration , this analysis shows how it plays the role of an apparent mass. In fact, the equation of motion becomes

$$\left(1 + \left(\frac{\delta}{l}R\right)^2\right)\tilde{Y}''(\tilde{t}) = 1 \tag{16}$$

that shows the retarding effect of the lift. In future work, the effect of the shear layer reflections on the apparent mass term M in (16) will be obtained, first, for the linear approximate boundary condition and secondly, for the previously mentioned nonlinear and free boundary effects.

A cross-check of the imaging procedure will use the mapping

$$W = -2\cot^{-1} Z$$

which maps the region exterior to the circle representing the cross section of the cylindrical store to the inside of a rectangle in the upper half of the W plane. This

mapping is a combination of a logarithmic and bilinear transformation and provides two pencils of biaxal circles to form a bipolar network in which the store is embedded. The vertical sides of the rectangle correspond to the two sides of the cut y axis between 0 and $i(a-R)$ in the Z plane. Its top is the perimeter of the circle and its bottom is the origin Z =0. The shear layer maps into the origin W =0. The W transformed Neumann problem can then be solved by an eigenfunction expansion. This solution will be also used to cross check the solution of the boundary element methods for nonlinear problems.

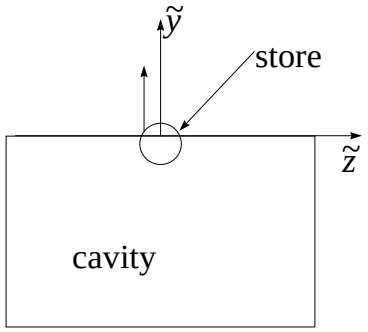

Fig. 9 Cross flow projection of cylindrical store transiting shear layer.

Shalaev, Fedorov and Malmuth in recent analyses [3] describe initial approaches to treat coupling with the shear layer and the walls as well shear layer transit interactions with pitch. The transit interactions are shown schematically in Fig. 9. The corresponding inner solutions [3] allow us to calculate the vertical evolution of the body center of inertia and pitch angle history for the separation to subsonic or transonic streams. Comparisons of that analysis with subsonic experimental data were obtained in a test program that we implemented with M. Hites and D. Williams of the Illinois Institute of Technology (IIT) and reported in [4]. A major innovation tailored to our analytical thrust was to perform ***free drop*** experiments in a wind tunnel as contrasted to the ***Captive Trajectory Support (CTS)*** system typically used in store tests. The latter intrinsically assumes pseudo-steady conditions and is confounded by largely unknown sting interactions. We chose to avoid these issues as well as to tailor the experiments to complement our theoretical studies. Generic store shapes consisting of tail-finned ogive cylinders were tested. The experimental arrangement was a cavity cut-out in the IIT wind tunnel simulating a weapons bay as shown in Fig. 10. A special compression actuator system was developed to almost instantaneously and cleanly release the stores. A variety of runs were made, for various values of the ballistic parameter and other variables. Store configurations associated with these variations are shown in Fig. 11. The models were caught by a series of nets downstream of the test section. Linear and angular trajectories were obtained by post-processing of ultra fast photographic scans of the trajectories. Initial comparisons with this database and our theoretical results given in the next section.

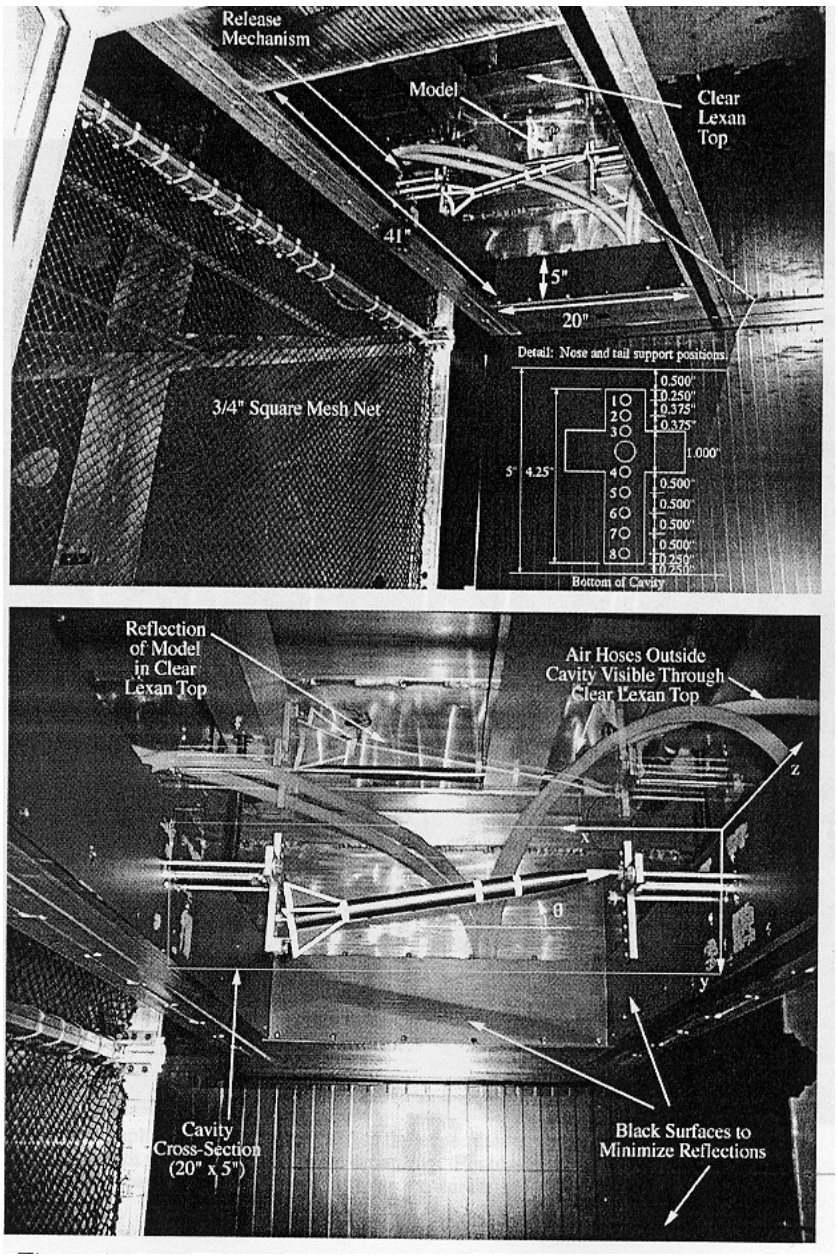

Fig. 10 Top: wide –angle of view of 41″×20″×5″ cavity in installed in the IIT National Diagnostic Facility, cables and hoses can be seen since top panel is transparent, bottom: close-up of the cavity showing the perspective of the side view camera.

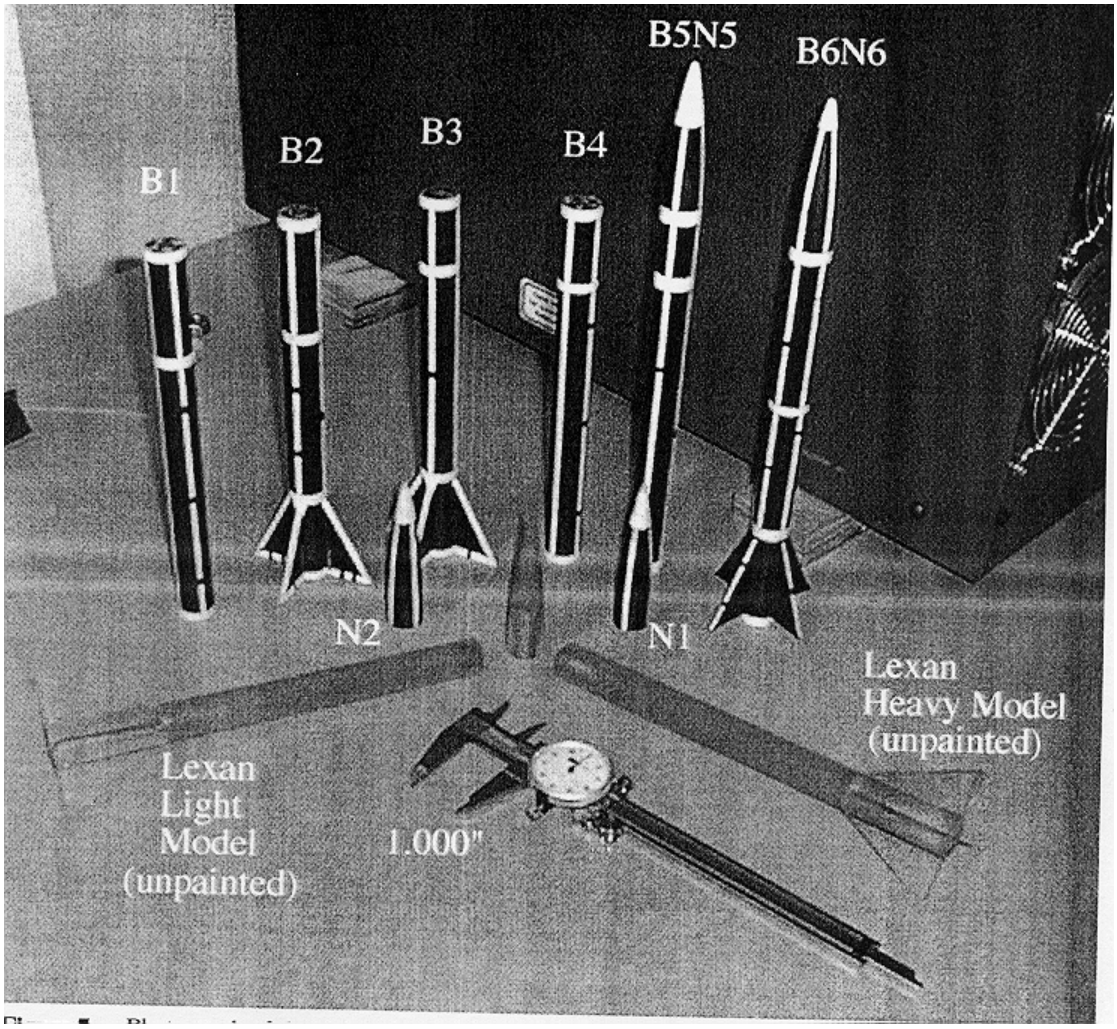

Fig. 11 Stores selected for tests.

6. Comparison with experiment

Theoretical model

To bound the problem we have initially used a simplified model for calculations of the lift force and the pitching moment. Within the cavity we consider just a free drop. When the body intersects the shear layer we use the exact solution of the potential equation. When the body is completely outside the cavity, we use a simple solution, which does not account for interaction with cavity walls and shear layer.

Experimental data

We consider the following cases reported in [4]:

1. Light finless model B4N2 with the initial angle of attack $\theta_0 = 0$ at freestream Mach number $M = 0.182$. Experimental data of this case are shown in Fig. 42 of [4]. In this case pitching is very small and the angle of attack is close to zero.

2. Light finless model B4N2 with the initial angle of attack $\theta_0 = 0$ at freestream Mach number $M = 0.225$. Experimental data of this case are shown in Fig. 45 of [4]. The model rotates inside the cavity and attains the pitch angle about $\theta = 11^o$ by the moment of interaction with the shear layer (time is about 0.1 s). Then the model pitches down to $\theta = -2.4^o$.

We did not consider cases for the heavy finless model B1N1 because they are weakly sensitive to the flow. In these cases the model trajectory is well defined by a simple free drop approximation.

Comparison

Figure 12a shows the vertical coordinate *y* of the gravity center as a function of time *t* for Case 1 (see also Fig. 42 of [4]). Figure 12b shows the pitch angle θ as a function of time *t*. In this case aerodynamic force and moment are small. The theoretical curve *y(t)* (solid line) is close to the free drop approximation (dashed line) as well as experimental data (points). The theory predicts the general trends of the pitch angle history $\theta(t)$. As soon as the model gets in the free stream, the pitch angle starts to oscillate.

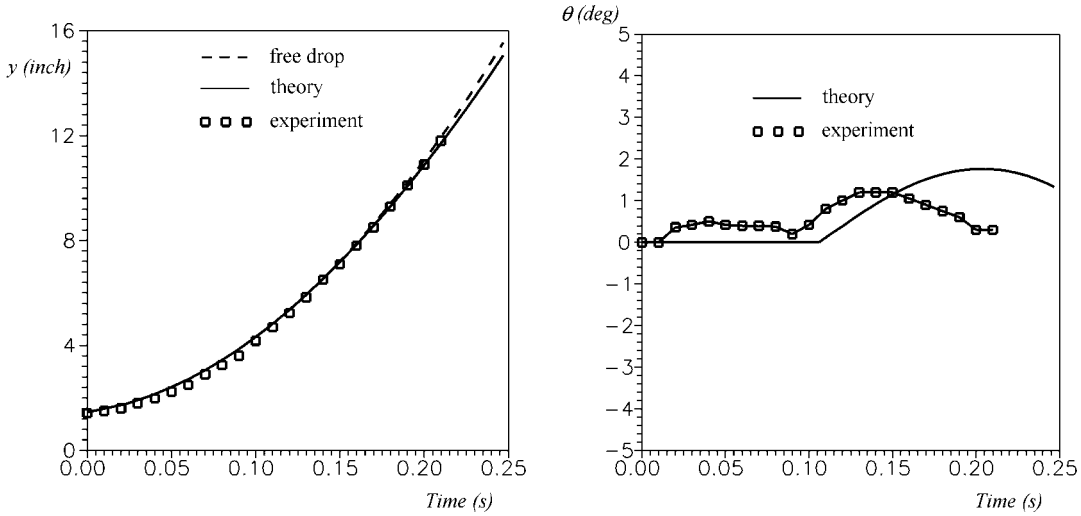

a) b)

Fig. 12 Comparison of theory (solid line) with experimental data of Case 1 (symbols).

Figure 13 shows the vertical coordinate *y* of the gravity center as a function of time *t* for Case 2 (see also Fig. 45 of Ref. [3]). Figure 13b shows the pitch angle θ as a function of time *t*. In this case aerodynamic force and moment cause a detectable effect. The theoretical curve *y(t)* (solid line) is closer to the experimental data (symbols) than the free drop approximation (dashed line). The model attains the pitching angular velocity inside the cavity. We think this pitch is due to the release mechanism. In our calculations we consider the inside motion as a free drop. Starting from the moment of the intersection between the model surface and the shear layer, we perform our calculations using experimental values of the pitch angle as an initial condition. It is seen that our theoretical model predicts the pitch down effect observed in experiment.

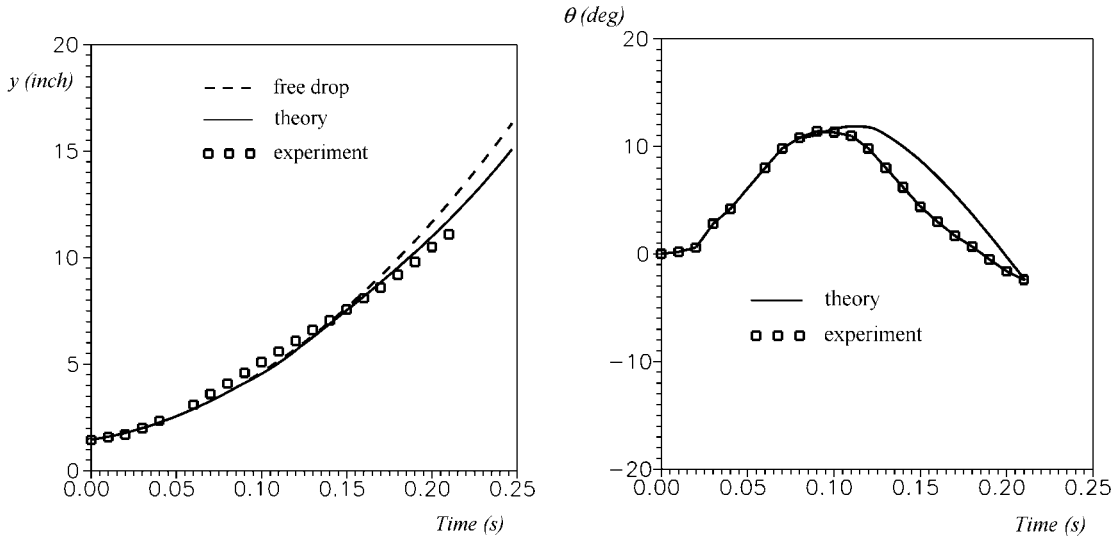

a) b)

Fig. 13 Comparison of theory (solid line) with experimental data of Case 2 (symbols).

7. Transonic regime

In order to calculate the drag force we analyze the outer asymptotic region, $r\tau^2 = O(1)$. In scope of the slender body theory [5], the transonic regime differs from the subsonic regime in this region only. In Ref. [6], we showed that the outer flow is induced by sources distributed along the body axis. Their intensity depends on the cavity span and characteristics of the inner solution. As an example, we consider the body separation from a flat plate that models the store separation from a wing of a transport aircraft. In this case, the outer problem corresponds to the flow over the body of revolution with the cross-sectional area distribution $A_e(x) = 2A(x)$, where $A(x)$ is body cross-sectional area. Accounting for this relation we can calculate the wave drag, which is a function of the transonic Karman-Guderley similarity parameter only. The friction drag is modeled using the empirical method of Schlichting-Grenwill [7]. The pressure drag is calculated by integration of the inner-field pressure over the body surface. The lift force and pitch moment are calculated using the theoretical model described above. Figures 14a and 14b show the body trajectories for the freestream Mach number $M_\infty = 0.999$ for zero initial vertical and angular velocities. It is seen that for an initial angle of attack $\alpha_0 = 6^\circ$, the body moves up to re-contact the wing (see Fig. 14a). For $\alpha_0 = -6^\circ$ (Fig. 14b), the body can escape from the wing. Its angle of attack oscillates with growing amplitude. This indicates weak dynamic instability of the store under consideration.

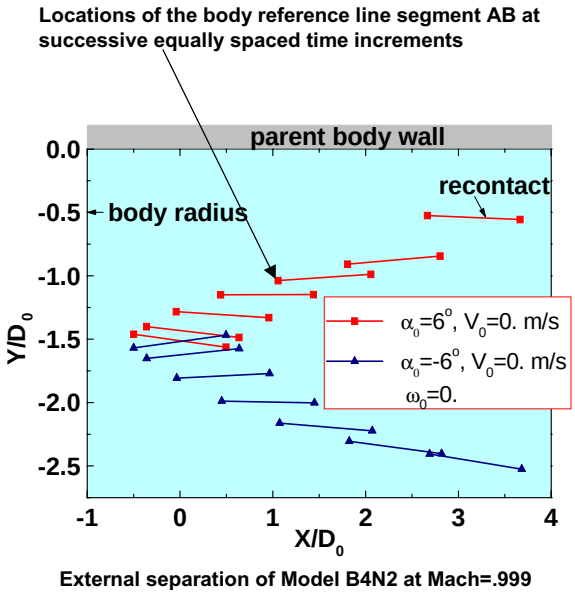

Fig. 14a Trajectories at various initial angle of attack, freestream Mach number 0.999.

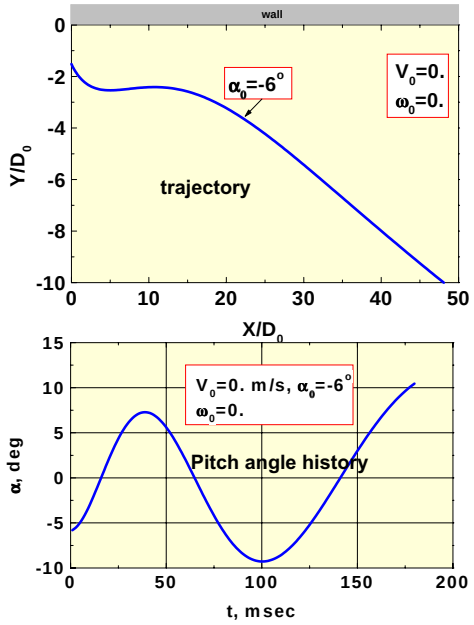

Fig. 14b Center of gravity trajectory and pitch angle history at initial angle of attack $\alpha_0 = 6^\circ$.

8. Conclusions

Combined asymptotics and numerics (CAN) give an insightful picture of shear layer cavities and provide a means of quickly visualizing the flow pattern within them. It appears that the recirculating flow can be modeled with inviscid approximations of the viscous flow for many practical cases. For bodies transiting the shear layer of such

cavities such as in store separation, much of the details such as the modification of the apparent mass effect due to the shear layer can be obtained from cross flow approximation-inner solutions from slender body theory. These tools are now being extended to transonic flows. Initial studies show that the inner solution of the incompressible case plays a significant role in the flow structure for the transonic one.

Acknowledgments

Some portions of the research discussed herein were sponsored by Boeing and Rockwell IR&D. Other portions of this effort was supported by the Air Force Office of Scientific Research, Air Force Materials Command under Contract Nos. F49620-92-C-0006, F49620-96-C-0004 and F49620-99-C-0005. The U.S. government is authorized to reproduce and distribute reprints for government purposes, notwithstanding any copyright notation thereon. The views and conclusions herein are those of the authors and should not be interpreted as necessarily representing the official policies or endorsements, either expressed, or implied of the Air Force Office of Scientific Research or the U.S. government.

References

1. Durand, W. (ed.) *Aerodynamic Theory*, Volume II, Vol. 2, 18, pp. 208-211, 1943.
2. Shalaev, V. and Fedorov, A., "Flow Field Near a Body Transiting a Free Stream," Rockwell interim report to N. Malmuth (1997.)
3. Malmuth, N. D, Shalaev, V.I., and Fedorov, A.V., "Separation of Thin Body of Revolution from Rectangular Cavities," Rockwell Science Center, 1999, Report No. SCNM99-1.
4. Hites, M. and D. Williams, "Photographic Investigation of the Dynamics of an Ogive Model Near a Cavity at Subsonic Mach Numbers," Draft of the Final Report, Fluid Dynamics Research Center, Illinois Institute of Technology, January 18, 1998.
5. Cole, J.D. *Perturbation Methods in Applied Mathematics*. Waltham. Massachusetts. 1968.
6. Shalaev, V. and Fedorov, A., "On store separation problem at transonic speeds," Rockwell interim report to N. Malmuth (June, 2000.)
7. Schlichting, H., *Boundary Layer Theory*, McGrow-Hill Company, 1987.

Paper: 37
Author: Dr. Malmuth

Question by Mr. Sacher: Was only drop considered, or ws ejection through the shear layer also considered?

Answer: For the analysis in the paper, only drops were considered. However, our treatment can be generalized to handle ejection.

Question 2: Is the configurational impact of the carrier aircraft taken in account?

Answer: The large-scale flow on the airplane was not included in the analysis. However, this large-scale flow we believe is an "outer" weak perturbation of our solution, which is a local "inner" solution in the terminology of matched asymptotic expansions. In future work, this outer solution will be considered.

Question by Mr. Jeune: Is it possible to extrapolate or use your method in supersonic flow conditions?

Answer: Absolutely. We are working on this.

Question by Dr. Khalid: You showed very good comparisons between your theoretical prediction and experiment. How did the CFD computations fair in this comparison?

Answer: We did not attempt any CFD computations yet. We intend to make this comparison in the future.

Question by Mr. Verhaagen: Would your method help optimize the interior shapes of the cavity?

Answer: Yes, we think it will be very helpful for this purpose.